

## Ultracritical Floquet Non-Fermi Liquid

Li-kun Shi<sup>1,2,\*</sup>, Oles Matsyshyn<sup>3,\*</sup>, Justin C. W. Song<sup>3</sup>, and Inti Sodemann Villadiego<sup>1</sup>

<sup>1</sup>*Institut für Theoretische Physik, Universität Leipzig, Brüderstraße 16, 04103, Leipzig, Germany*

<sup>2</sup>*Center for Quantum Matter, School of Physics, Zhejiang University, Hangzhou 310058, China*

<sup>3</sup>*Division of Physics and Applied Physics, School of Physical and Mathematical Sciences, Nanyang Technological University, Singapore 637371*

(Received 22 October 2024; revised 24 January 2025; accepted 23 April 2025; published 15 May 2025)

We demonstrate that periodically driven Fermions coupled to simple bosonic baths have steady state occupations of Floquet Bloch bands that generically display nonanalyticities at certain momenta that resemble the Fermi surfaces of equilibrium non-Fermi liquids. Remarkably these nonequilibrium Fermi surfaces remain sharp even when the bath is at finite temperature, leading to critical power-law decaying correlations at finite temperature, a phenomenon with no analog in equilibrium. We also show that generically there is in-gap current rectification for clean metals lacking inversion symmetry, and explain why this occurs universally regardless of the details of collisions.

DOI: 10.1103/PhysRevLett.134.196401

**Introduction**—The transitivity of thermal equilibrium or zeroth law of thermodynamics [1] encodes a remarkable universality of thermal baths in equilibrium, namely, a system coupled to a bath always thermalizes toward the same macroscopic state regardless of the details of the bath. However, for nonequilibrium settings the details of the bath matter. In this Letter we will demonstrate a dramatic example of this by showing that periodically driven fermions coupled to a boson bath have a steady state occupation function with nonanalyticities at certain special momenta that resemble the Fermi surfaces of a non-Fermi liquid state [see Fig. 1(c) and Refs. [2–4]]. This sharply contrasts with the case when they are coupled to a fermion bath, which displays a Fermi-Dirac staircase occupation with multiple jumps, and behaves like a Fermi liquid, as we have recently demonstrated in Refs. [5,6] (for related studies see also Refs. [7–12]).

We will also show that, remarkably, these nonanalyticities remain sharp even when the boson bath is at finite temperature, and thus these Floquet non-Fermi liquid Fermi surfaces do not suffer from thermal smearing, leading to correlations that decay like power laws at long distances even at finite temperature. This behavior, which we refer to as “ultracritical,” has no analog in equilibrium, where Fermi surfaces of Fermi and non-Fermi liquids invariably

smear at finite temperature and correlations decay exponentially at long distances.

**Floquet-Boltzmann equation**—We consider a fermionic system ( $S$ ) coupled to a bosonic bath ( $B$ ), described by the Hamiltonian [see Fig. 1(a)]

$$\hat{H}(t) = \hat{H}_S(t) + \hat{H}_B + \hat{H}_{SB} + \text{H.c.}, \quad (1)$$

where  $\hat{H}_S(t) = \sum_{\alpha\beta} \langle \alpha | \hat{h}_t | \beta \rangle \hat{a}_\alpha^\dagger \hat{a}_\beta$ ,  $\hat{H}_B = \sum_q \hbar \omega_q \hat{b}_q^\dagger \hat{b}_q$ , and  $\hat{H}_{SB} = \sum_{q,\nu,\eta} \langle \nu | \hat{\chi}_q | \eta \rangle \hat{b}_q \hat{a}_\nu^\dagger \hat{a}_\eta$ .  $\hat{h}_t$  and  $\hat{\chi}_q$  are the system single particle Hamiltonian matrix and its coupling matrix to the mode  $q$  of the bath,  $\hat{a}_\alpha^\dagger$ ,  $\hat{a}_\alpha$  ( $\hat{b}_q^\dagger$ ,  $\hat{b}_q$ ) are fermionic (bosonic) creation and annihilation operators for state  $|\alpha\rangle$  (mode  $q$ ). The bath is in thermal equilibrium with Bose-Einstein occupation  $N_q = 1/(e^{\beta\hbar\omega_q} - 1)$  and temperature  $k_B T_0 = 1/\beta$ , but the system can be driven out of

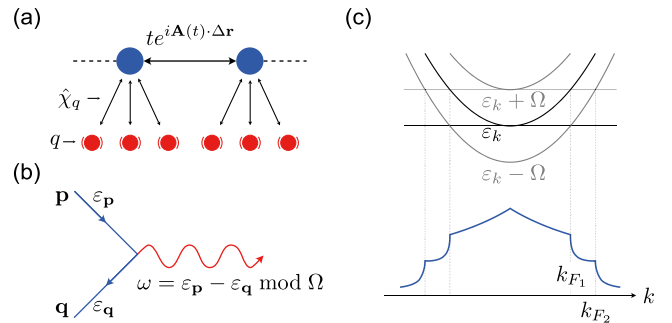


FIG. 1. (a) Schematic of a periodically driven tight-binding model (blue) coupled to boson modes (red) [see Eq. (1)], enabling (b) Floquet-Umklapp processes [see Eq. (6)] and resulting in (c) Floquet non-Fermi liquid Fermi surfaces  $k_{F_n}$  at intersections of band edges and its Floquet copies.

\*These authors contributed equally to this work.

Published by the American Physical Society under the terms of the Creative Commons Attribution 4.0 International license. Further distribution of this work must maintain attribution to the author(s) and the published article's title, journal citation, and DOI.

equilibrium via the time dependence of  $\hat{h}_t$  (hence the subscript  $t$ ). Starting from the full density matrix for the system and bath,  $\hat{\eta}_t$ , and following the analysis of Raichev and Basko [13] for weak system-bath coupling (see Sec. A of [14]), we arrive at a quantum kinetic equation for the system one-body density matrix  $\rho_{\gamma\delta} \equiv \text{Tr}[\hat{\eta}_t \hat{a}_\delta^\dagger \hat{a}_\gamma]$ ,

$$\hbar \partial_t \hat{\rho}_t + i[\hat{h}_t, \hat{\rho}_t] = \hat{I}_t^e + \hat{I}_t^a, \quad (2)$$

where  $\hat{I}_t^e$  and  $\hat{I}_t^a$  are, respectively, the emission and absorption collision operators, which are given by

$$\begin{aligned} \hat{I}_t^e = & \frac{1}{\hbar} \sum_q (N_q + 1) \int_{-\infty}^t dt' e^{i\omega_q(t-t')} [\hat{U}(t, t') \\ & \times (\hat{\rho}_{t'} \hat{\chi}_q (1 - \hat{\rho}_{t'}) + \hat{\rho}_{t'} \text{tr}[\hat{\rho}_{t'} \hat{\chi}_q]) \hat{U}(t', t), \hat{\chi}_q^\dagger] + \text{H.c.}, \end{aligned} \quad (3)$$

where  $\hat{U}$  is the system unitary evolution matrix in the absence of coupling to the bath. The absorption operator  $\hat{I}_t^a$  can be obtained from  $\hat{I}_t^e$  by substituting  $N_q + 1 \rightarrow N_q$ ,  $\omega_q \rightarrow -\omega_q$ ,  $\hat{\chi} \rightarrow \hat{\chi}^\dagger$  [13]. We will apply this general formalism to investigate the steady states of Floquet Bloch bands. For simplicity we consider tight-binding models with one site per unit cell (i.e., no Berry phases) periodically driven by a spatially uniform electric field, with an associated vector potential  $\mathbf{A}(t) = \mathbf{A}(t + T)$ . Therefore, the system Hamiltonian is  $\hat{h}_t = \sum_{\mathbf{k}} \epsilon(\mathbf{k} - \mathbf{A}(t)) |\mathbf{k}\rangle \langle \mathbf{k}|$ . We couple each site,  $\mathbf{r}$ , of the tight-binding model to its own collection of local boson modes, namely, the label for boson modes can be written as  $q = (\mathbf{r}, \lambda)$ , where  $\lambda$  labels the different boson modes coupled to each site [see Fig. 1(a)]. The frequency of the boson modes is site independent and only depends on  $\lambda$ , namely,  $\omega_q = \omega_\lambda$ . We consider the limit where  $\lambda$  becomes dense and the density of states (DOS) of the bath,  $\nu_B(\omega) = \sum_\lambda \delta(\omega - \omega_\lambda)$ , approaches a continuous function, which we will specify in the coming sections. Moreover, we take the boson modes to be coupled to the on-site fermion density, namely the coupling matrix is simply the projector onto a system site  $\hat{\chi}_q = \chi_0 |\mathbf{r}\rangle \langle \mathbf{r}|$ , and  $\chi_0$  is the same for all boson modes.

Starting from Eq. (2), one can show that in the limit of weak coupling to the bath ( $\chi_0 \rightarrow 0$ ) the one-body density matrix of the fermionic system approaches the steady state (see Sec. A of [14]),

$$\rho_t = \sum_{\mathbf{k}} f_{\mathbf{k}} |\mathbf{k}\rangle \langle \mathbf{k}|, \quad (4)$$

where the occupations,  $f_{\mathbf{k}}$ , are determined by the solutions of the time-independent Floquet-Boltzmann equation

$$\sum_{\mathbf{q}} (f_{\mathbf{q}} W_{\mathbf{q} \rightarrow \mathbf{p}} \bar{f}_{\mathbf{p}} - f_{\mathbf{p}} W_{\mathbf{p} \rightarrow \mathbf{q}} \bar{f}_{\mathbf{q}}) = 0, \quad \bar{f}_{\mathbf{p}} \equiv 1 - f_{\mathbf{p}}, \quad (5)$$

where the scattering rates are given by

$$\begin{aligned} W_{\mathbf{q} \rightarrow \mathbf{p}} &= 2\pi |\chi_0|^2 \sum_l \Phi_{\mathbf{q}, \mathbf{p}}^{(l)} (\epsilon_{\mathbf{q}} - \epsilon_{\mathbf{p}} + l\Omega), \\ \Phi_{\mathbf{q}, \mathbf{p}}^{(l)} &= \sum_{l'} |\varphi_{l', \mathbf{p}} \varphi_{l'+l, \mathbf{q}}^*|^2, \end{aligned} \quad (6)$$

where  $\epsilon_{\mathbf{k}}$  and  $\varphi_{l, \mathbf{k}}$  are, respectively, the Floquet band energy and  $l$ th harmonic of the wave function, i.e., the solution of the Schrödinger equation for  $h_t$  is  $|\psi_{\mathbf{k}}(t)\rangle = \sum_l e^{-i(\epsilon_{\mathbf{k}} + l\Omega)t} \varphi_{l, \mathbf{k}} |\mathbf{k}\rangle$ . The function  $S$ , which encapsulates both emission and absorption processes, is given by

$$S(\omega) = [N_b(|\omega|) + \Theta(\omega)] \nu_B(|\omega|) \quad (7)$$

and plays a crucial role in the properties of the solutions of this Floquet-Boltzmann equation. The argument of  $S$  can be interpreted as the energy of a boson that is emitted (absorbed) to (from) the bath when it is positive (negative), and therefore we see that the scattering behaves as if there was energy conservation modulo  $\Omega$  (Floquet-Umklapp) [see Fig. 1(b)]. Similar Floquet-Boltzmann equations have been employed in previous studies [7, 15–17]. For concreteness we will focus on the case of a parabolic band dispersion in one and two dimensions,

$$\epsilon_{\mathbf{k}}(t) = [\mathbf{k} - \mathbf{A}(t)]^2 / 2m, \quad (8)$$

where  $A(t) = A_0 \sin(\Omega t + \phi_0)$  in 1D and in 2D we will restrict to circularly polarized light,  $\mathbf{A}(t) = A_0 [\sin(\Omega t + \phi_0), \sin(\Omega t + \phi_0 \pm \pi/2)]$ , so that the steady state has rotational symmetry in order to simplify the numerical solutions (but our main conclusions remain qualitatively valid for arbitrary polarization). The Floquet energies and wave functions for this problem are shown in Sec. E of [14].

Notice that while the density matrix in Eq. (4) is time-independent in canonical momentum basis,  $\mathbf{k}$ , physical quantities will generically oscillate periodically since they depend on the mechanical momentum  $\mathbf{k} - \mathbf{A}(t)$ . This steady state is an example of a periodic Gibbs ensemble (PGE) [18–21], which does not arise from many-body self-thermalization but rather from the coupling to a bath. We have recently shown that the steady state when the system is coupled to a fermion bath is another PGE with a Fermi-Dirac staircase occupation with multiple jumps that behaves like a Fermi liquid at low temperatures [5, 6]. As we will show, however, the solutions of Eq. (5) lead to a dramatically different PGE where the occupation  $f_{\mathbf{k}}$  does not feature jumps, but instead displays higher order non-analyticities. These effectively behave as the Fermi surfaces of a non-Fermi liquid, and we refer to this state “Floquet non-Fermi liquid.” Remarkably, these nonanalyticities remain sharp even when the bath is at finite temperature, a property we will call “ultracritical.” Our findings can be viewed as establishing that these nonanalyticities appear for an infinitesimally weak electron-boson interaction ( $\chi_0 \rightarrow 0$ ), in contrast to the equilibrium, where non-Fermi liquid

behavior typically emerges from strong interactions [2–4]. In Sec. I of [14] we provide a rigorous demonstration that these nonanalyticities remain robust after including electron-electron collisions (as derived in Ref. [15]) in Eq. (5). While this is reminiscent to the setting in equilibrium where critical boson modes lead non-Fermi liquid behavior, e.g., within the Hertz-Millis framework [22,23], we caution that our states should not be confused with equilibrium non-Fermi liquids, since nonequilibrium conditions are crucial in our setting.

*Floquet non-Fermi liquid with Ohmic bath*—We start by considering an Ohmic bosonic bath characterized by a density of states that vanishes linearly at low frequency,

$$\nu_B^{\text{ohm}}(\omega) = (c_1\omega + c_2\omega^2 + \dots)\Theta(\omega). \quad (9)$$

We solve the Floquet-Boltzmann Eq. (5) numerically [24] by keeping the scattering matrix to the second order of  $A_0^2$ . We have found that  $f_{\mathbf{k}}$  has nonanalyticities at  $|\mathbf{k}| = k_{Fn}$  given by [see Fig. 2(a)]

$$k_{Fn}^2/2m = n\Omega, \quad n = 1, 2, \dots \quad (10)$$

that are the ‘‘Floquet Fermi surfaces’’ (FFSs) [25]. The size of FFSs is independent of the fermion density and thus generally different from the size of the equilibrium Fermi surface. The origin of these nonanalyticities can be traced back to three crucial ingredients: (a) the absence of detailed balance in the scattering rates from Eq. (6); (b) the existence of a nonanalyticity in the DOS of the Floquet energies, which for a parabolic band is the DOS edge from the band bottom at  $\mathbf{k} = 0$ ; (c) the existence of a nonanalyticity of the  $S$  function from Eq. (7), which for the Ohmic bath occurs at  $\omega = 0$ . The idea is that states near an FFS, ( $|\mathbf{k}| \approx k_{Fn}$ ), can scatter into or from those near the bottom of the band ( $\mathbf{k} \approx 0$ ) while absorbing or emitting

bosons from the bath with negligibly small energy  $\omega \approx 0$  [see Figs. 1(b) and 1(c)], which becomes allowed in the Floquet setting because energy is conserved only modulo  $\Omega$  (Floquet-Umklapp). We have found that when the driving amplitude is small ( $|\mathbf{E}| \ll \Omega^2/v_F$ ), the nonanalyticity with  $n = 1$  is the strongest one (see Fig. 2).

The degree of non-analyticity depends on space dimensionality ( $d = 1, 2$ ). In Sec. D of [14], we prove that for the Ohmic bath the second derivative of  $f(k)$  exhibits non-analyticities of the form:  $d^2f/dk^2 = (d^2f/dk^2)_{\text{reg}} + \sum_n b_n (k - k_{Fn})^{(d-2)/2} \Theta(k - k_{Fn})$ . Here  $b_n$  is a constant, and  $(d^2f/dk^2)_{\text{reg}}$  includes the analytic part and weaker non-analyticities. Namely, these correspond to a square-root kink in  $df/dk$  in 1D, and a jump in  $d^2f/dk^2$  in 2D as illustrated in Fig. 2(a).

*Floquet non-Fermi liquid with gapped bath*—In order to illustrate that the nonanalyticities of the  $S$  function from Eq. (7) affect the location of the FFSs, we now consider a bosonic bath with a gap ( $\Delta$ ) in its DOS, given by

$$\nu_B^{\text{gap}}(\omega) = \Theta(\omega - \Delta), \quad \Delta > 0. \quad (11)$$

We have verified that the behavior remains qualitatively similar if the above Theta function is replaced by other similar functions with a single discontinuity at  $\omega = \Delta$ , but we will focus on the above case Eq. (11) for simplicity. Interestingly, in this case the nonanalyticities of  $f_{\mathbf{k}}$  are found at  $|\mathbf{k}| = k_{Fn,s}$  given by [see Fig. 2(b)]

$$k_{Fn,s}^2/2m = n\Omega + s\Delta, \quad (12)$$

where  $n, s$  can be any integers as long as the right-hand side is positive. We have observed that for weak amplitudes the strongest nonanalyticities are those with indices  $(n, s) \in \{(1, 1), (1, -1), (0, 1)\}$ . We will focus here on characterizing primarily those with  $(n, s) = (1, \pm 1)$ , which involve nontrivial Floquet-Umklapp scattering. These nonanalyticities are more pronounced in the gapped bath compared to the Ohmic case, and appear in the first derivative of the occupation function [see Fig. 2(b)]  $df/dk = (df/dk)_{\text{reg}} + \sum_{n,s} a_{n,s} (k - k_{Fn,s})^{(d-2)/2} \Theta(k - k_{Fn,s})$ , where  $d$  is the dimensionality, and  $a_{n,s}$  is the strength of the nonanalyticity (see Sec. D of [14] for proof). Figure 2(b) shows that  $a_{n=1,s=\pm 1}$  decays as  $1/T_0$  with bath temperature. Furthermore, for weak drivings,  $a_{n=1,s=-1}$  scales as  $A_0^2$ , while  $a_{n=1,s=+1}$  as  $A_0^4$  (see Sec. F of [14]).

*Friedel oscillations and particle-hole continuum*—To further substantiate the analogy between these nonanalyticities and Fermi surfaces of a non-Fermi liquid, we will show that they give rise to phenomena that are often seen as fingerprints of the presence of Fermi surfaces. We begin by illustrating that density correlations display power-law decaying oscillations analogous to Friedel oscillations. The pair-correlation function of the fluid,  $g(\mathbf{r}_1, \mathbf{r}_2, t)$ ,

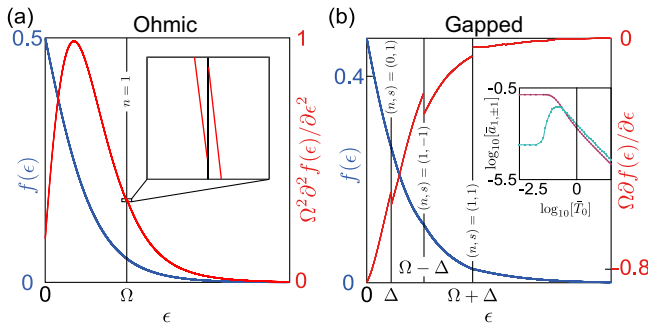


FIG. 2. Steady state occupation and FFSs for 2D parabolic bands coupled to (a) Ohmic and (b) gapped baths at finite temperature. The occupation (blue) and derivatives (red) are plotted as functions of  $\epsilon = k^2/2m$ . Inset (b) shows temperature  $\bar{T}_0 = k_B T_0/\Omega$  dependence of the amplitude of nonanalyticity  $\bar{a}_{n=1,s=1} = \Omega a_{n=1,s=1}$  (green) and  $\bar{a}_{n=1,s=-1} = \Omega a_{n=1,s=-1}$  (purple). Parameters used:  $c_1/c_2\Omega = 3$ ,  $\Delta/\Omega = 3/10$ ,  $A_0/\sqrt{6m\Omega} = 1/5$ , particle density  $n_0/(2m\Omega) = 3/13$ , bath temperatures  $\bar{T}_0 = 3/10$ .

measures the probability at time  $t$  of finding a particle at location  $\mathbf{r}_2$  given that another one is at  $\mathbf{r}_1$ . We find that (see details in Sec. G of [14]) translational invariance and time independence of the one-body density matrix in canonical momentum basis [see Eq. (2)] lead to  $g(\mathbf{r}_1, \mathbf{r}_2, t) = g(0, \mathbf{r}_2 - \mathbf{r}_1, 0) \equiv g(\mathbf{r}_2 - \mathbf{r}_1)$ , and that this function is related to the real space Fourier transform,  $\tilde{f}(\mathbf{r})$ , of the momentum occupation,  $f(\mathbf{k})$ , as follows  $g(\mathbf{r}) = 1 - [\tilde{f}(\mathbf{r})/\tilde{f}(0)]^2$ . Moreover, in 2D the isotropy of  $f_{\mathbf{k}}$  under circularly polarized light leads to a pair correlation that only depends on the distance  $|\mathbf{r}_2 - \mathbf{r}_1|$ . For the gapped bath we find the asymptotic behavior ( $|\mathbf{r}| \rightarrow \infty$ )

$$\tilde{f}(\mathbf{r}) \approx -\sum_{n,s} \frac{(\pi a_{n,s})(k_{F_{n,s}}/2)^{\frac{d-1}{2}}}{(\pi|\mathbf{r}|)^{\frac{2d+1}{2}}} \sin\left(k_{F_{n,s}}|\mathbf{r}| + \frac{\pi}{4}\right), \quad (13)$$

where  $n, s$  labels different Fermi surfaces. Therefore, each Floquet Fermi surface contributes to a Friedel-like oscillation of  $g(\mathbf{r})$  with period  $2k_{F_{n,s}}$  and decaying with power  $1/|\mathbf{r}|^{2d+1}$ , as we illustrate in Sec. G of [14]. Remarkably, the above power-law correlations remain even when the bath is at finite temperature because the Floquet Fermi surface remains sharp, which is the behavior that we call ultracritical. This contrasts with the Friedel oscillations in equilibrium whose amplitude decays as  $1/|\mathbf{r}|^{d+1}$  at zero temperature but exponentially at finite temperatures [26] due to the thermal smearing of the Fermi surface.

Another manifestation of a sharp Fermi surface is the existence of nonanalyticities of dynamical correlations at frequencies,  $\omega$ , and wave vectors,  $\mathbf{q}$ , that match energies and wave vectors of particle-hole excitations arbitrarily close to the Fermi surface, i.e., at the edge of the particle-hole continuum. In equilibrium the boundary of this particle-hole continuum smears out at finite temperatures due to the thermal smearing of the Fermi surface [26]. To investigate the presence of a particle-hole continuum in our setting, we consider the unequal-time density correlation function  $C(\mathbf{r}_1, t_1; \mathbf{r}_2, t_2) = \langle n(\mathbf{r}_1, t_1)n(\mathbf{r}_2, t_2) \rangle - \langle n(\mathbf{r}_1, t_1) \rangle \langle n(\mathbf{r}_2, t_2) \rangle$ . Translational invariance leads to  $C(\mathbf{r}_1, t_1; \mathbf{r}_2, t_2) = C(\mathbf{r}_1 - \mathbf{r}_2, t_1; 0, t_2)$ . Because of the periodic driving this function depends not only on  $t = t_1 - t_2$ , but also periodically on  $\bar{t} = (t_1 + t_2)/2$ . Therefore, for simplicity, we will focus on the correlation averaged over one period, defined as  $\bar{C}(\mathbf{r}, t) = \int_0^T C(\mathbf{r}, t + t_2; 0, t_2) dt_2/T$ . Its Fourier transform is (see Sec. H of [14])

$$\bar{C}(\mathbf{q}, \omega) = \frac{1}{V} \sum_{\mathbf{k}, l} f_{\mathbf{k}+\mathbf{q}} \bar{f}_{\mathbf{k}} \Phi_{\mathbf{k}, \mathbf{k}+\mathbf{q}}^{(l)} \delta(\varepsilon_{\mathbf{k}} - \varepsilon_{\mathbf{k}+\mathbf{q}} - l\omega). \quad (14)$$

For an FFS with radius  $k_F$  we have found that this function displays nonanalyticities at finite bath temperatures for [see Fig. 3(a)],

$$\omega = \pm k_F |\mathbf{q}|/m \pm |\mathbf{q}|^2/2m + l\Omega, \quad (15)$$

where  $l = 0$  are the same values expected for a parabolic Fermi surface of radius  $k_F$  in equilibrium [26], and  $l \neq 0$  are Floquet copies. The angular dependence of  $\bar{C}(\mathbf{q}, \omega)$  in 2D is nontrivial and is discussed in Sec. H of [14].

*Current rectification*—Recently, we demonstrated that the steady state of a metal coupled to a fermion bath sustains a nonzero rectified electric current even when it is driven by monochromatic light whose frequency lies in its optical gap [5,27], offering a counterexample to claims that such current should generally vanish [28–32]. Here, we will argue that this conclusion is general and that in particular remains valid for boson baths. The steady state current for a single band model averaged over one period is [5]

$$\mathbf{j} = \int d^d k f_{\mathbf{k}} \partial_{\mathbf{k}} \varepsilon_{\mathbf{k}} / (2\pi)^d, \quad (16)$$

where  $\varepsilon_{\mathbf{k}} = \int_0^T \varepsilon(\mathbf{k} - \mathbf{A}(t)) dt/T$  is the Floquet energy. Crucially, in the Floquet setting the steady state occupation  $f_{\mathbf{k}}$  cannot be expressed as a function of the Floquet energy,  $\varepsilon_{\mathbf{k}}$ , alone. If that was the case (i.e., in equilibrium), then  $\mathbf{j}$  could be expressed as the integral of a total derivative over the Brillouin zone and would always vanish. However, the lack of detailed balance combined with the fact that the scattering rates in Eq. (5) depend explicitly on Floquet wave functions and scattering matrix elements prohibit expressing  $f_{\mathbf{k}}$  as a local function of  $\varepsilon_{\mathbf{k}}$  (in contrast to equilibrium). Therefore, one expects that generically, as long as there is no  $\mathbf{k} \rightarrow -\mathbf{k}$  symmetries, the steady state would have a nonzero rectified current, regardless of details of the collisions or the precise nature of the bath. In particular, the nonanalyticities that we have found in the current work, or the multiple steps found in our previous study with fermion baths [6], are not crucial for the existence of the in-gap rectified current.

To illustrate this explicitly, we consider a 1D Bloch band without  $k \rightarrow -k$  symmetry with dispersion  $\varepsilon_k = -t_1 \cos(a_0 k) - t_2 \sin(2a_0 k)$ , driven by  $A(t) = A_0 \sin(\Omega t)$ . Figure 3(b) shows the current in the steady state when the system is coupled to the bosonic bath and also the fermionic bath from Refs. [5,6]. We see that in both cases the rectified current is nonzero.

*Generalizations and discussion*—We have observed the appearance of nonanalyticities in the fermion occupation of Floquet bands coupled to boson baths that resemble Fermi surfaces in non-Fermi liquids. While we have illustrated this in detail for a parabolic band model, our results are quite general. In fact, we can now conjecture a general criterion for the location of the FFSs. Suppose that the Floquet spectrum has a nonanalyticity in its DOS at a Floquet energy  $\varepsilon_*$ , e.g., arising from a local band minimum. Suppose that the DOS of the boson bath has a nonanalyticity at some energy  $\omega_*$ . Then we expect the presence

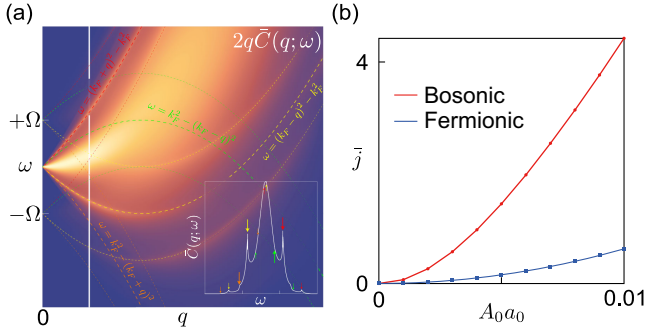


FIG. 3. (a) Correlator  $2q\bar{C}(q; \omega)$  from Eq. (14) for 1D parabolic model coupled to a gapped bath with  $T_0/\Omega = 1/5$  and  $\Delta/\Omega = 1/100$ . Thick (thin) dashed lines are for  $l = 0$  ( $l = \pm 1$ ) nonanalyticities [see Eq. (15)]. The inset shows the cut (white) at  $q/\sqrt{m\Omega} = 2/3$ , with big (small) arrows being crossings between the thick (thin) dashed lines and the cut. Parameters used:  $A_0/\sqrt{m\Omega} = 4/5$ , and the particle density  $n_0/\sqrt{m\Omega} = 1/2$ . (b) Rectification current density  $\bar{j} = j/10^{-4}t_1$  as a function of the driving amplitude  $A_0$  for a 1D Bloch band coupled to an Ohmic bosonic bath or an ideal fermionic bath using Eqs. (5) and (16). Parameters:  $t_2/t_1 = 1/2$ ,  $\Omega/t_1 = 2/3$ ,  $k_B T_0/t_1 = 1/100$ , and particle density  $n_0 a_0 = \sqrt{1/3}$ .

of a collection of Floquet Fermi surfaces associated with these nonanalyticities parametrized by two integers ( $n, s$ ) at the following momenta:

$$\varepsilon_{\mathbf{k}} = \varepsilon_* + n\Omega + s\omega_*, \quad (17)$$

where  $\varepsilon_{\mathbf{k}}$  is the Floquet dispersion and  $\Omega$  is the driving frequency. We have shown that these nonanalyticities remain sharp even when the boson bath is at finite temperature, leading to finite temperature Friedel-like oscillations of the density correlations, and sharp particle-hole continua edges, which are often viewed as characteristic phenomena of sharp Fermi surfaces.

We have also demonstrated that the steady state occupation of a Floquet band coupled to a boson bath generally has a rectified current. This is a general conclusion independent of the details of collisions, and provides a general demonstration that there will be finite current rectification in ideal inversion-breaking metals illuminated by monochromatic light even when the frequency lies within its optical gap, as we have previously argued [5,6,27].

Our Letter illustrates how the steady states of open and driven quantum fluids can retain intriguing quantum characteristics. Let us summarize the key experimental conditions to realize such true Floquet steady states of electrons in materials. The visibility of Floquet effects is controlled by the amplitude of Floquet harmonics, which typically scale as  $|\varphi_{l=\pm 1}|^2 \sim (ev_F|\mathbf{E}|/\hbar\Omega^2)^2$  (see Sec. E of [14]). Therefore, in the clean limit it is advantageous to have as low a frequency as possible, so that a small electric

field amplitude is sufficient to reach sizable values of these harmonics and consequently there is less heating from the continuous irradiation. But this frequency should also be larger than the inverse electron lifetime; otherwise, Floquet effects are also smeared. For example, in a clean material with a lifetime of tens of picoseconds, radiations with frequencies on the order of 100 GHz (i.e., microwaves) would be desirable.

The above conditions are similar to those used to observe a variety of beautiful phenomena in high-mobility two-dimensional electron gases [33] such as microwave-induced resistance oscillations (MIROs). MIROs are reminiscent of quantum oscillations under magnetic fields, but with a period consistent with a Fermi surface of area  $\Omega$ , such as the one we have found for  $n = 1$  from Eq. (10). Therefore, there is a tantalizing possibility that an ultra-critical Floquet non-Fermi liquid state is realized in these materials. However, we note that we have also shown that a Floquet Fermi liquid could also give rise to MIROs over the same period [6], and other mechanisms for MIROs have been proposed [33]. This allows us to reiterate that for out-of-equilibrium settings, the details of the bath and relaxation mechanisms matter much more than in equilibrium. Thus, further work is needed to fully clarify the precise nature of steady states in these systems and to solve open puzzles of MIROs (see, e.g., Ref. [34]). We would also like to note that an interesting analogue of MIRO has been reported in graphene at terahertz frequencies in Ref. [44].

Although there have been several interesting experimental studies of Floquet physics with midinfrared ultrafast optical techniques [35–43], we believe that realizing true Floquet steady states in clean materials with nontrivial electronic structures remains a largely open and remarkably fertile ground for discovering new physics. As we have emphasized, a strategy to reach such nontrivial quantum true Floquet steady states is to drive clean materials with much lower frequencies.

*Acknowledgments*—We would like to thank Matthias Thamm, Achim Rosch, Mark Rudner, Takashi Oka, Aris Alexandradinata, and Sebastian Diehl for stimulating and helpful discussions. We acknowledge support by the Deutsche Forschungsgemeinschaft (DFG) through research grant Project No. 542614019, No. 518372354, No. 555335098 (IS) and Singapore Ministry of Education under its Academic Research Fund Tier 2 Grant No. MOE-T2EP50222-0011 (JCWS) and Tier 3 Grant No. MOE-MOET32023-0003 Quantum Geometric Advantage (JCWS).

- 
- [1] M. Kardar, *Statistical Physics of Particles* (Cambridge University Press, Cambridge, England, 2007).
  - [2] T. Giamarchi, *Quantum Physics in One Dimension* (Clarendon Press, New York, 2003), Vol. 121.

- [3] T. Senthil, Critical Fermi surfaces and non-Fermi liquid metals, *Phys. Rev. B* **78**, 035103 (2008).
- [4] C. M. Varma, Z. Nussinov, and W. Van Saarloos, Singular or non-Fermi liquids, *Phys. Rep.* **361**, 267 (2002).
- [5] O. Matsyshyn, J. C. W. Song, I. S. Villadiego, and L. K. Shi, Fermi-Dirac staircase occupation of Floquet bands and current rectification inside the optical gap of metals: An exact approach, *Phys. Rev. B* **107**, 195135 (2023).
- [6] L. K. Shi, O. Matsyshyn, J. C. W. Song, and I. S. Villadiego, Floquet Fermi liquid, *Phys. Rev. Lett.* **132**, 146402 (2024).
- [7] K. I. Seetharam, C.-E. Bardyn, N. H. Lindner, M. S. Rudner, and G. Refael, Controlled population of Floquet-Bloch states via coupling to Bose and Fermi baths, *Phys. Rev. X* **5**, 041050 (2015).
- [8] Y. V. Nazarov and Y. M. Blanter, *Quantum Transport: Introduction to Nanoscience* (Cambridge University Press, Cambridge, England, 2009).
- [9] P. Tien and J. Gordon, Multiphoton process observed in the interaction of microwave fields with the tunneling between superconductor films, *Phys. Rev.* **129**, 647 (1963).
- [10] R. Kumari, B. Seradjeh, and A. Kundu, Josephson-current signatures of unpaired Floquet Majorana fermions, *Phys. Rev. Lett.* **133**, 196601 (2024).
- [11] M. M. Asmar and W.-K. Tse, Impurity screening and Friedel oscillations in Floquet-driven two-dimensional metals, *J. Phys. Condens. Matter* **34**, 315602 (2022).
- [12] T. Le, R. Jiang, L. Tu, R. Bian, Y. Ma, Y. Shi, K. Jia, Z. Li, Z. Lyu, X. Cao *et al.*, Inverse-current quantum electro-oscillations in a charge density wave insulator, *Phys. Rev. B* **109**, 245123 (2024).
- [13] F. T. Vasko and O. E. Raichev, *Quantum Kinetic Theory and Applications* (Springer, New York, 2005).
- [14] See Supplemental Material at <http://link.aps.org/supplemental/10.1103/PhysRevLett.134.196401>, which includes Ref. [13], for (A) derivation of the collision integral, (B) collision integral for Floquet systems, (C) general analysis of nonanalyticities, (D) analytical analysis of  $S$  function for different types of baths, (E) parabolic models used in the main text, (F) Floquet-Boltzmann equation for the parabolic models, (G) equal time pair-correlation function for the Floquet non-Fermi liquid, (H) density noise correlation function for the Floquet non-Fermi liquid, and (I) persistence of nonanalyticities in the presence of electron-electron interactions.
- [15] M. Genske and A. Rosch, Floquet-Boltzmann equation for periodically driven Fermi systems, *Phys. Rev. A* **92**, 062108 (2015).
- [16] I. Esin, M. S. Rudner, G. Refael, and N. H. Lindner, Quantized transport and steady states of Floquet topological insulators, *Phys. Rev. B* **97**, 245401 (2018).
- [17] K. I. Seetharam, C.-E. Bardyn, N. H. Lindner, M. S. Rudner, and G. Refael, Steady states of interacting Floquet insulators, *Phys. Rev. B* **99**, 014307 (2019).
- [18] A. Lazarides, A. Das, and R. Moessner, Periodic thermodynamics of isolated quantum systems, *Phys. Rev. Lett.* **112**, 150401 (2014).
- [19] A. Lazarides, A. Das, and R. Moessner, Equilibrium states of generic quantum systems subject to periodic driving, *Phys. Rev. E* **90**, 012110 (2014).
- [20] A. Lazarides, A. Das, and R. Moessner, Fate of many-body localization under periodic driving, *Phys. Rev. Lett.* **115**, 030402 (2015).
- [21] V. Khemani, A. Lazarides, R. Moessner, and S. L. Sondhi, Phase structure of driven quantum systems, *Phys. Rev. Lett.* **116**, 250401 (2016).
- [22] J. A. Hertz, Quantum critical phenomena, *Phys. Rev. B* **14**, 1165 (1976).
- [23] A. J. Millis, Effect of a nonzero temperature on quantum critical points in itinerant fermion systems, *Phys. Rev. B* **48**, 7183 (1993).
- [24] A. Pal, F. Holtorf, A. Larsson, T. Loman, F. Schaefer, Q. Qu, A. Edelman, C. Rackauckas *et al.*, Nonlinearsolve.jl: High-performance and robust solvers for systems of nonlinear equations in Julia, [arXiv:2403.16341](https://arxiv.org/abs/2403.16341).
- [25] We also see a non-analyticity  $\mathbf{k} = 0$  associated with  $n = 0$ , but here we focus on those with finite radius.
- [26] G. Giuliani and G. Vignale, *Quantum Theory of the Electron Liquid* (Cambridge University Press, Cambridge, England, 2008).
- [27] L. K. Shi, O. Matsyshyn, J. C. W. Song, and I. S. Villadiego, Berry-dipole photovoltaic demon and the thermodynamics of photocurrent generation within the optical gap of metals, *Phys. Rev. B* **107**, 125151 (2023).
- [28] V. Belinicher, E. Ivchenko, and G. Pikus, Transient photocurrent in gyrotropic crystals, *Sov. Phys. Semicond.-USSR* **20**, 558 (1986).
- [29] Y. Onishi, H. Watanabe, T. Morimoto, and N. Nagaosa, Effects of relaxation on the photovoltaic effect and possibility for photocurrent within the transparent region, *Phys. Rev. B* **106**, 235110 (2022).
- [30] L. E. Golub and M. M. Glazov, Raman photogalvanic effect: Photocurrent at inelastic light scattering, *Phys. Rev. B* **106**, 205205 (2022).
- [31] E. Ivchenko, Y. B. Lyanda-Geller, and G. Pikus, Magneto-photogalvanic effects in noncentrosymmetric crystals, *Ferroelectrics* **83**, 19 (1988).
- [32] S. S. Pershoguba and V. M. Yakovenko, Direct current in a stirred optical lattice, *Ann. Phys. (Amsterdam)* **447**, 169075 (2022).
- [33] I. A. Dmitriev, A. D. Mirlin, D. G. Polyakov, and M. A. Zudov, Nonequilibrium phenomena in high Landau levels, *Rev. Mod. Phys.* **84**, 1709 (2012).
- [34] Q. Shi, P. D. Martin, A. T. Hatke, M. A. Zudov, J. D. Watson, G. C. Gardner, M. J. Manfra, L. N. Pfeiffer, and K. W. West, Shubnikov-de Haas oscillations in a two-dimensional electron gas under subterahertz radiation, *Phys. Rev. B* **92**, 081405(R) (2015).
- [35] Y. Wang, H. Steinberg, P. Jarillo-Herrero, and N. Gedik, Observation of Floquet-Bloch states on the surface of a topological insulator, *Science* **342**, 453 (2013).
- [36] J. W. McIver, B. Schulte, F.-U. Stein, T. Matsuyama, G. Jotzu, G. Meier, and A. Cavalleri, Light-induced anomalous Hall effect in graphene, *Nat. Phys.* **16**, 38 (2020).
- [37] J.-Y. Shan, M. Ye, H. Chu, S. Lee, J.-G. Park, L. Balents, and D. Hsieh, Giant modulation of optical nonlinearity by Floquet engineering, *Nature (London)* **600**, 235 (2021).

- [38] S. Aeschlimann, S. A. Sato, R. Krause, M. Chávez-Cervantes, U. De Giovannini, H. Hübener, S. Forti, C. Coletti, K. Hanff, K. Rossnagel *et al.*, Survival of Floquet–Bloch states in the presence of scattering, *Nano Lett.* **21**, 5028 (2021).
- [39] S. Zhou, C. Bao, B. Fan, H. Zhou, Q. Gao, H. Zhong, T. Lin, H. Liu, P. Yu, P. Tang *et al.*, Pseudospin-selective Floquet band engineering in black phosphorus, *Nature (London)* **614**, 75 (2023).
- [40] X. Zhang, T. Carbin, A. B. Culver, K. Du, K. Wang, S.-W. Cheong, R. Roy, and A. Kogar, Light-induced electronic polarization in antiferromagnetic Cr<sub>2</sub>O<sub>3</sub>, *Nat. Mater.* **23**, 790 (2024).
- [41] N. Bielinski, R. Chari, J. May-Mann, S. Kim, J. Zwettler, Y. Deng, A. Aishwarya, S. Roychowdhury, C. Shekhar, M. Hashimoto *et al.*, Floquet–Bloch manipulation of the Dirac gap in a topological antiferromagnet, *Nat. Phys.* **21**, 458 (2025).
- [42] M. Merboldt, M. Schüler, D. Schmitt, J. P. Bange, W. Bennecke, K. Gadge, K. Pierz, H. W. Schumacher, D. Momeni, D. Steil *et al.*, Observation of Floquet states in graphene, [arXiv:2404.12791](https://arxiv.org/abs/2404.12791).
- [43] D. Choi, M. Mogi, U. De Giovannini, D. Azoury, B. Lv, Y. Su, H. Hübener, A. Rubio, and N. Gedik, Direct observation of Floquet–Bloch states in monolayer graphene, [arXiv:2404.14392](https://arxiv.org/abs/2404.14392).
- [44] E. Mönch, D. A. Bandurin, I. A. Dmitriev, I. Y. Phinney, I. Yahniuk, T. Taniguchi, K. Watanabe, P. Jarillo-Herrero, and S. D. Ganichev, Observation of terahertz-induced magneto-oscillations in graphene, *Nano Lett.* **20**, 5943 (2020).